Current Biology *18*, 56–62, January 8, 2008 ©2008 Elsevier Ltd All rights reserved DOI 10.1016/j.cub.2007.11.066

Report

TORC1 Is Essential for NF1-Associated Malignancies

Cory M. Johannessen,[1,2,3] Bryan W. Johnson,[1,2,3] Sybil M. Genther Williams,[1,3] Annie W. Chan,[4,6] Elizabeth E. Reczek,[1,3] Ryan C. Lynch,[3,5] Matthew J. Rioth,[3,5] Andrea McClatchey,[6,7] Sandra Ryeom,[3,5] and Karen Cichowski[1,2,3,*]

[1]Genetics Division
Department of Medicine
Brigham and Women's Hospital
Boston, Massachusetts 02115
[2]Ludwig Center at Dana-Farber/Harvard Cancer Center and
[3]Harvard Medical School
Boston, Massachusetts 02115
[4]Department of Radiation Oncology
Massachusetts General Hospital (MGH)
Boston Massachusetts 02114
[5]Vascular Biology Program
Children's Hospital Boston
Boston, Massachusetts 02115
[6]MGH Center for Cancer Research and
[7]Department of Pathology
Harvard Medical School
Charlestown, Massachusetts 02129

Summary

Inactivating mutations in *NF1* underlie the prevalent familial cancer syndrome neurofibromatosis type 1 [1]. The *NF1*-encoded protein is a Ras GTPase-activating protein (RasGAP) [2]. Accordingly, Ras is aberrantly activated in *NF1*-deficient tumors; however, it is unknown which effector pathways critically function in tumor development. Here we provide in vivo evidence that TORC1/mTOR activity is essential for tumorigenesis. Specifically, we show that the mTOR inhibitor rapamycin potently suppresses the growth of aggressive NF1-associated malignancies in a genetically engineered murine model. However, in these tumors rapamycin does not function via mechanisms generally assumed to mediate tumor suppression, including inhibition of HIF-1α and indirect suppression of AKT, but does suppress the mTOR target Cyclin D1 [3]. These results demonstrate that mTOR inhibitors may be an effective targeted therapy for this commonly untreatable malignancy. Moreover, they indicate that mTOR inhibitors do not suppress all tumor types via the same mechanism, suggesting that current biomarkers that rely on HIF-1α suppression may not be informative for all cancers. Finally, our results reveal important differences between the effects of mTOR inhibition on the microvasculature in genetically engineered versus xenograft models and indicate that the former may be required for effective preclinical screening with this class of inhibitors.

*Correspondence: kcichowski@rics.bwh.harvard.edu

Results and Discussion

NF1$^{-/-}$ MPNST Cell Lines Are Sensitive to Rapamycin

An important feature of NF1 is the development of malignant peripheral nerve sheath tumors (MPNSTs), which are highly aggressive and frequently metastasize [1]. Consequently, greater than 50% of patients with MPNSTs present with unresectable disease. Despite radiation and, in some cases, chemotherapy, inoperable tumors rapidly progress and are universally lethal [4]. As such, identifying an effective treatment for NF1, in particular MPNSTs, is critical.

We and others have demonstrated that *NF1* inactivation results in the aberrant activation of the mTOR pathway, raising the possibility that NF1-associated tumors may be dependent on increased mTOR signaling [5, 6]. To test this hypothesis we first examined the effects of rapamycin on human and murine MPNST cell lines. All MPNST cell lines were potently inhibited by low doses of rapamycin with IC_{50} values $\leq$10 nM (Figures S1A and S1B available online) [6]. In contrast, wild-type Schwann cells, fibroblasts, and unrelated rapidly growing human tumor cell lines were not similarly sensitive to rapamycin (Figures S1B and S1C). Consistent with previous reports, low doses of rapamycin effectively suppressed mTOR activity in "insensitive" cell types, indicating that *NF1*-deficient MPNSTs are particularly dependent on mTOR activity and not that mTOR is more easily suppressed in these cells (Figures S1C and S1D) [7]. Notably, the sensitivity of NF1-deficient MPNSTs is similar to that of VHL-deficient kidney tumor cell lines, a tumor type that is currently showing promising results in clinical trials with mTOR inhibitors [7, 8]. Finally, we found that rapamycin functions by triggering a growth arrest of MPNST cells rather than apoptosis or senescence (Figure S2).

Rapamycin Rapidly Inhibits Tumor Growth in a Genetically Engineered MPNST Mouse Model

To test the requirement for mTOR in tumorigenesis in vivo and assess the therapeutic utility of rapamycin, we utilized a genetically engineered spontaneous tumor model of NF1. Mice carrying compound mutations in the *Nf1* and *p53* tumor suppressors on the same chromosome (NPcis animals) develop aggressive MPNSTs that are histologically indistinguishable from human tumors with an average latency of 5 months [9, 10]. These lesions develop as a result of somatic loss of the wild-type *Nf1* and *p53* alleles, and therefore are also genetically similar to human MPNSTs. Animals with palpable tumors (approximately 300 mm^3) were treated with 5 mg/kg rapamycin, as described in the Experimental Procedures section. Control NPcis mice died on average in 12.2 days (Figure 1A), and tumors grew 9.7-fold (Figures 1B and 1D). In contrast, rapamycin potently suppressed MPNST growth, resulting in only a 0.04-fold increase in size, and allowed the animals to

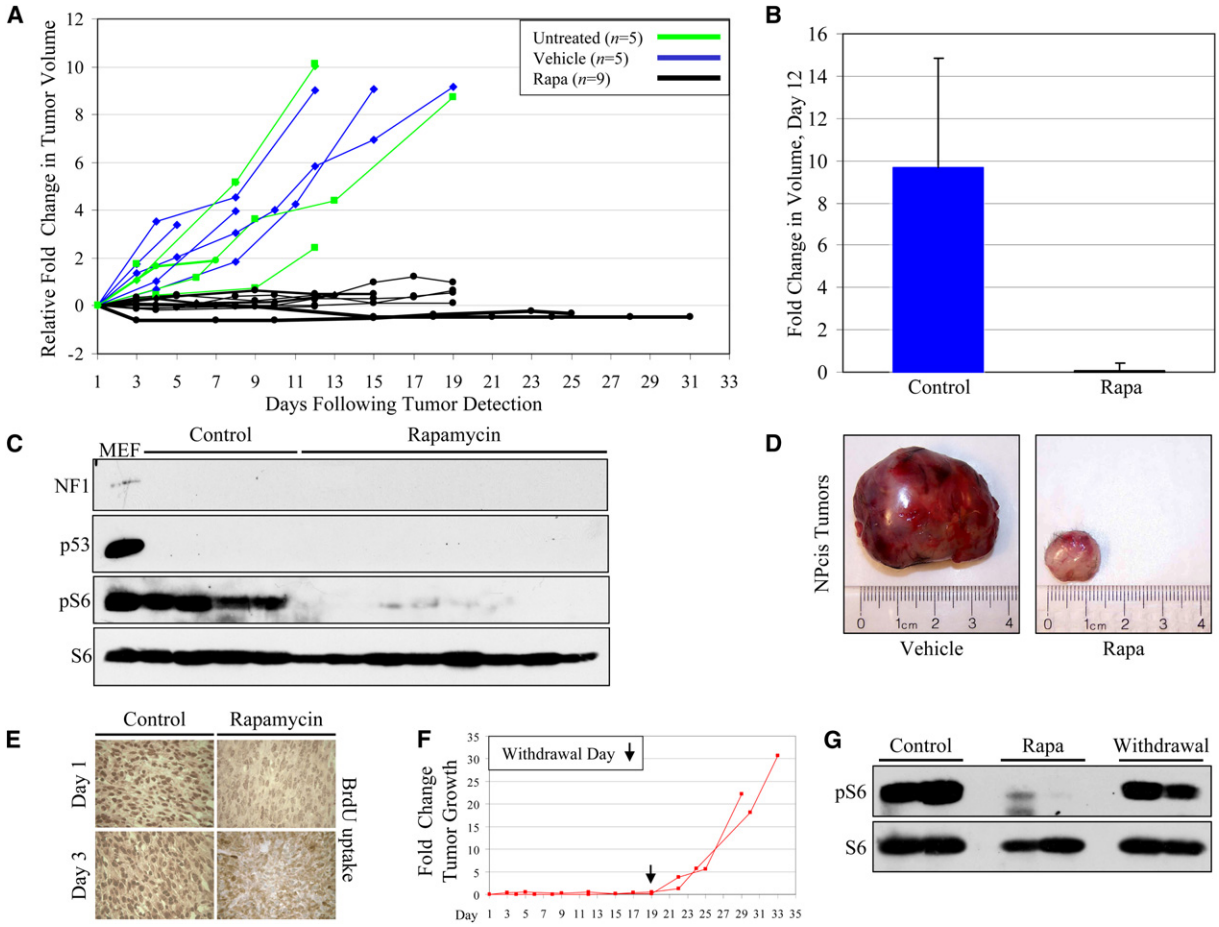

Figure 1. Rapamycin Rapidly Suppresses the Growth of NPcis MPNSTs In Vivo

(A) Growth kinetics of NPcis tumors left untreated (green), vehicle-treated (blue), and rapamycin-treated (black).

(B) Average n-fold change in tumor volume in NPcis mice after 12 days of treatment. Error bars represent the standard deviation (SD) calculated from the volume of six control and nine rapamycin-treated mice.

(C) Western-blot analysis of NPcis tumors. Abbreviations: NF1, neurofibromin; p53, TP53; pS6, ribosomal protein S6 phosphorylated at S235/236; S6, total ribosomal S6 protein.

(D) Photographs of NPcis tumors treated with either vehicle or rapamycin for 14 days.

(E) Immunohistochemical staining of incorporated BrdU in NPcis tumors, treated as indicated and exposed to BrDU for 4 hr.

(F) Growth kinetics of NPcis tumors during rapamycin treatment and after withdrawal of rapamycin (indicated by an arrow).

(G) Western-blot analysis of NPcis tumors.

survive. In no case did a rapamycin-treated animal die but, rather, animals were sacrificed for interim analysis. Thus, rapamycin has potent cytostatic effects on these highly aggressive malignancies.

Inhibition of S6 phosphorylation was observed in tumor and nontumor tissue, demonstrating that rapamcyin effectively suppressed the mTOR pathway in vivo (Figure 1C and Figure S3). Moreover, we found that rapamycin mediated its antitumor effects within 24 hr by potently suppressing proliferation, as assessed by BrDU incorporation in control and rapamycin-treated tumors (Figure 1E). Consistent with in vitro observations, markers of senescence were not detected (Figure S3 and data not shown). Tumor growth was dependent on continued exposure to rapamycin, as tumors re-exhibited S6 phosphorylation and resumed growing at a rate comparable to control-treated tumors after rapamycin removal (Figures 1F and 1G). Nevertheless, these data demonstrate that these aggressive tumors can be completely contained by an mTOR inhibitor. Notably, several other targeted agents have been shown to be clinically efficacious for other human malignancies by causing stable disease [11–13].

Effects of Rapamycin on the Microvasculature in a Genetically Engineered Tumor Model

To determine how rapamycin was functioning, we investigated several proposed mechanisms of action. In some xenograft models, rapamycin is thought to inhibit tumor growth via effects on the microvasculature rather than directly inhibiting tumor cell proliferation [14, 15]. However, the effects of rapamycin on the tumor microvasculature have never been examined in a genetically engineered model, which could be more stable than the nascent microvasculature of a xenograft. Both control and rapamycin treated tumors exhibited strong CD31 staining and a clearly defined microvasculature for the first 8 days (Figures 2A and 2B), suggesting that the immediate arrest induced by rapamycin was cell autonomous and not secondary to effects on the microvasculature.

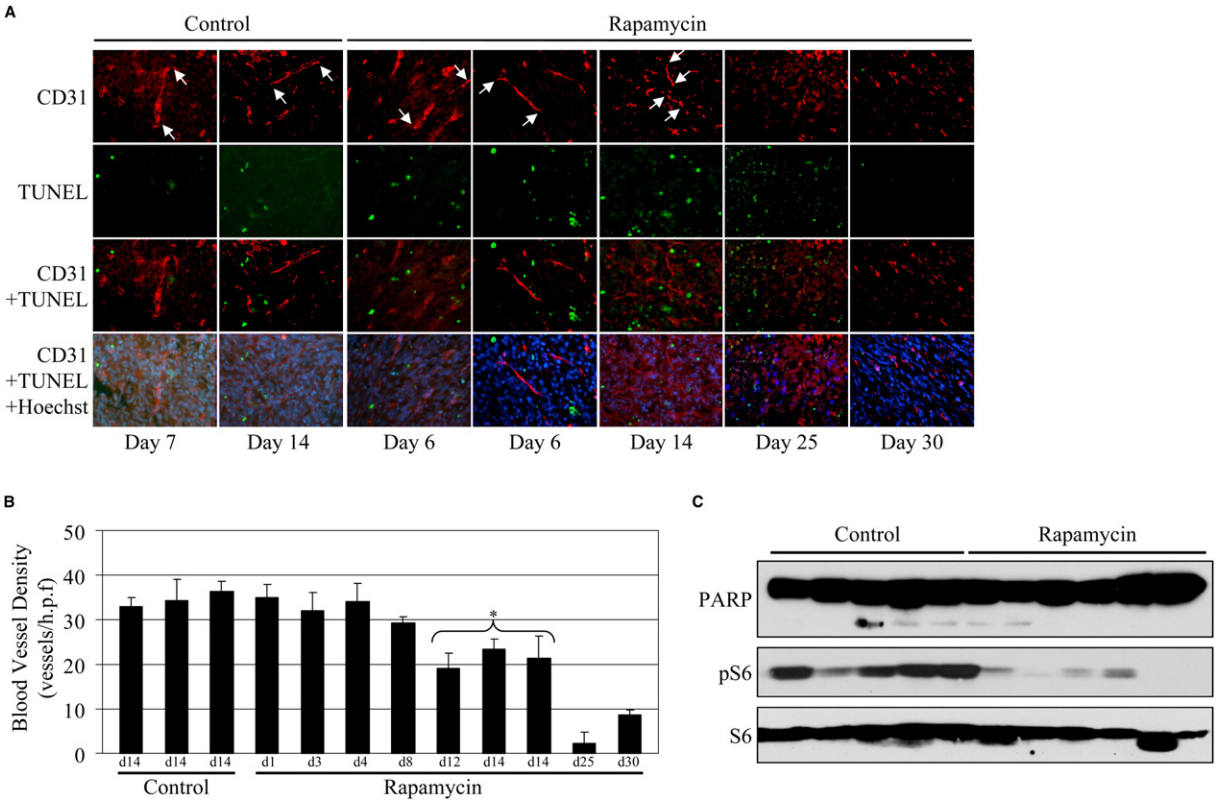

Figure 2. Rapamycin-Induced Growth Arrest Is Not a Consequence of Microvasculature Disruption in *Nf1*-Deficient MPNSTs

(A) Histological sections taken from NPcis MPNSTs. Endothelial cells were detected by indirect immunoflourescence with an antibody recognizing CD31 (red). Apoptotic cells are labeled by TUNEL staining (green), and nuclei are marked with Hoechst (blue).

(B) Quantitation of blood vessel density in NPcis MPNST histological sections stained with CD31, as described in (A). *p = 0.009. Error bars represent the SD of blood vessel density quantified from 27 microscopic fields per tumor.

(C) Western-blot analysis of NPcis tumors showing expression of full-length poly ADP ribose polymerase (PARP), phosphorylation of the ribosomal protein S6 at Ser235/236 (pS6), and total ribosomal S6 protein (S6).

Interestingly, however, after 14 days of treatment, rapamycin did lead to a 38% decrease in microvessel density, and by 25 days the microvasculature was significantly deteriorated (Figures 2A and 2B). Despite these observations, both control and rapamycin-treated tumors exhibited little apoptosis (Figures 2A and 2C), which did not increase with longer treatment times and appeared to occur outside the endothelial cell compartment.

These findings differ from observations in xenograft models, in which the microvasculature is rapidly disrupted by mTOR inhibitors and tumors often regress [14, 15]. This discrepancy may be due to differences in signals that maintain the relatively established vasculature of a spontaneously arising tumor versus those that support a developing xenograft. In this respect all xenograft tumors, irrespective of mTOR status, might be sensitive to the effects of mTOR inhibitors in ways that would not necessarily predict the therapeutic response of human tumors, a possibility consistent with previous findings [14, 15]. Therefore the stringency of this model further supports the potential translatability of these findings to humans and highlights the utility of using genetically engineered animals for preclinical studies, particularly with mTOR inhibitors. Nevertheless, long-term rapamycin treatment does ultimately disrupt the existing microvasculature, which may occur via combined effects on tumor and endothelial cells. In this regard perhaps mTOR inhibitors can be used to "reset" the angiogenic switch of sensitive tumor types, which could be clinically exploited.

Rapamycin Does Not Suppress HIF-1α in MPNSTs

mTOR has been shown to regulate the expression of HIF-1α [16, 17], and in some tumor types rapamycin is thought to mediate its effects by suppressing HIF-1α and HIF-1α transcriptional targets [8, 17]. Surprisingly, however, we found that rapamycin had no effect on HIF-1α protein (or transcript) levels in this tumor type (Figures 3A and 3B and data not shown). Consistent with the lack of an effect on HIF-1α expression, microarray-based profiling studies combined with gene set enrichment analysis (GSEA) revealed that rapamycin had no significant effect on a 30-member HIF-1α transcriptional target gene set in MPNSTs in vivo (p = 0.334). Real-time PCR analysis of a subset of genes was used to further confirm that rapamycin did not suppress HIF-1α transcriptional targets. (Figure 3C). Taken together, these results suggest that rapamycin does not mediate its growth inhibitory effects through suppression of HIF-1α or its target genes in this tumor type.

(18)F-fluorodeoxyglucose (FDG) uptake, quantified by positron emission tomography (PET) scans, has been proposed to serve as a pharmacodynamic readout of mTOR inhibition in some tumor types [8] and has been

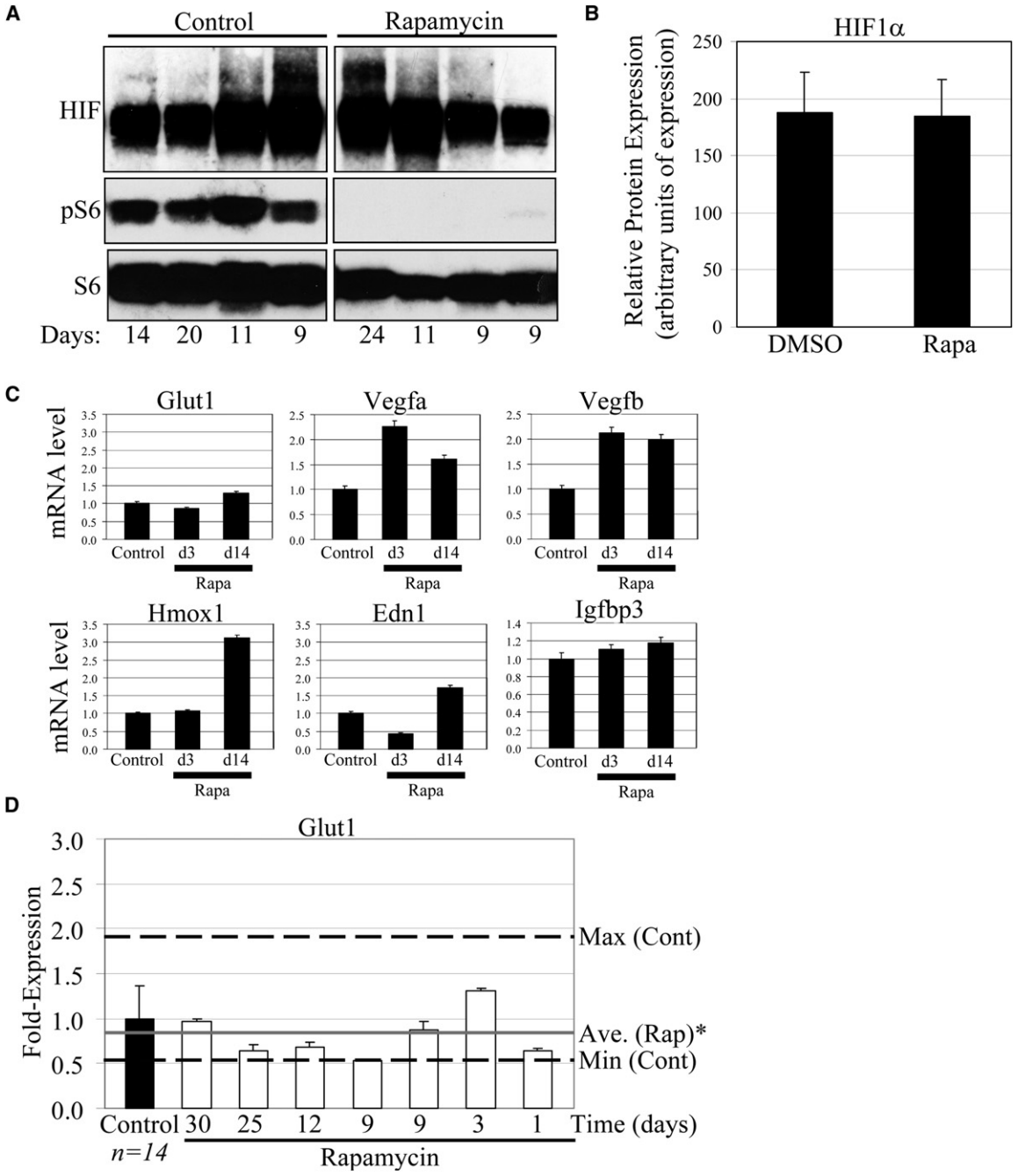

Figure 3. Rapamycin Treatment Does Not Affect HIF-1α Expression or Transcriptional Target Activation

(A) Western-blot analysis of HIF-1α protein expression in NPcis MPNSTs. "Days" indicates length of treatment.

(B) Quantification of HIF-1α protein expression relative to loading control in tumors (n = 6 in control and n = 7 rapamycin-treated tumors). Error bars represent the SD of relative protein expression quantified from immunoblots.

(C) Quantitative RT-PCR analysis of mRNA expression of six HIF-1α transcriptional targets in control or rapamycin-treated tumors. Error bars represent the SD of RT-PCR samples (n = 6 control and n = 7 rapamycin-treated tumors), performed in triplicate.

(D) Quantitative RT-PCR analysis of GLUT1 (Slc2a1) mRNA expression. mRNA was isolated from NPcis MPNSTs. Dashed lines (black) indicate maximum and minimum GLUT1 mRNA expression in control-treated tumors (n = 14). The solid line (gray) represents the average GLUT1 mRNA expression in rapamycin-treated tumors. *p = 0.162. Error bars from rapamycin-treated samples represent the SD of RT-PCR values performed in triplicate. Error bars from control tumors represent the SD of RT-PCR values from 14 independent tumors, performed in triplicate.

incorporated widely into clinical trials [18]. In part, the driving rationale is based on observations that mTOR inhibitors suppress HIF-1α in some tumor models (renal cell carcinoma and PIN) [8, 17] and, consequentially, suppress the target gene GLUT1, a glucose transporter that regulates FDG uptake [19]. To confirm that rapamycin was not suppressing GLUT1 in MPNSTs, real-time PCR was performed. Rapamycin did not significantly affect GLUT1 expression at any time point ranging from 3–30 days (Figure 3D). Therefore, based on these

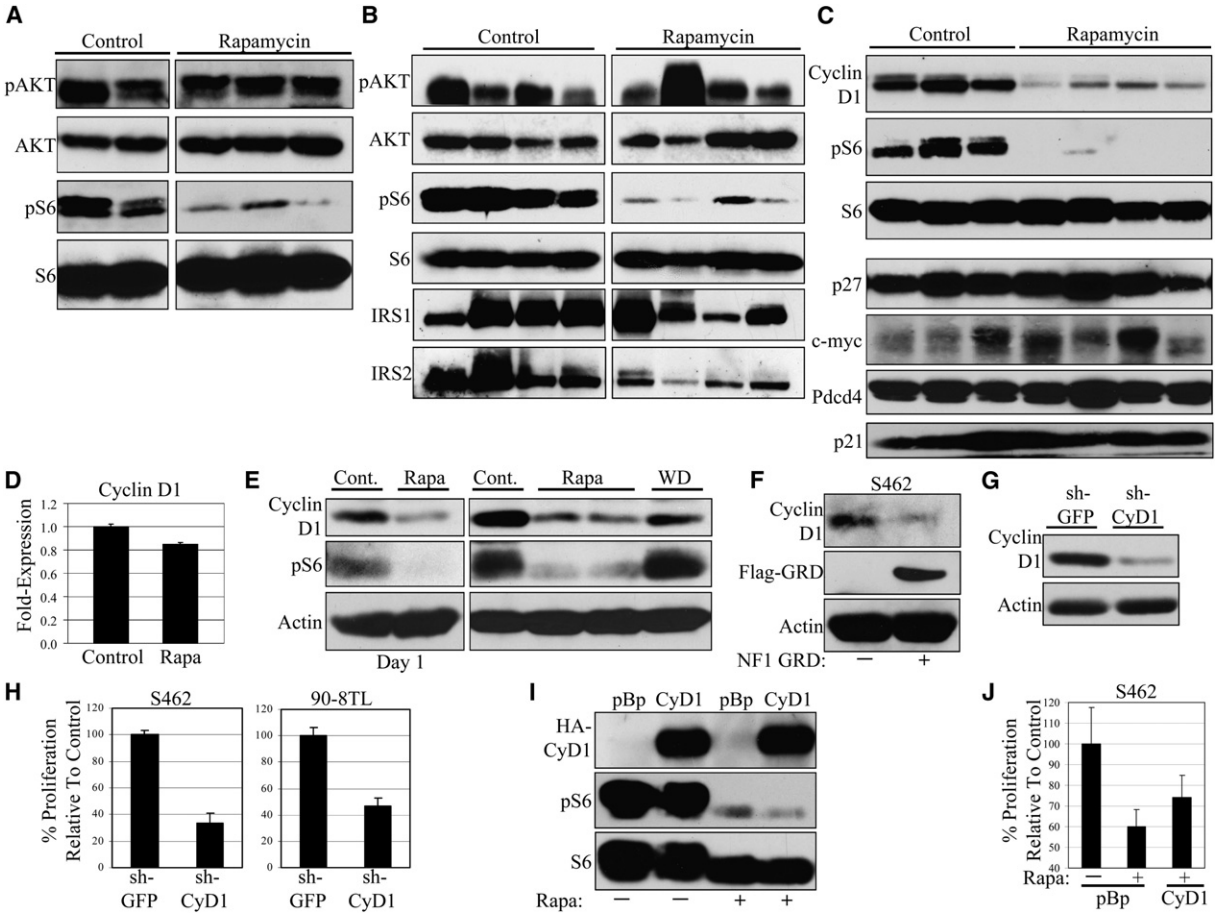

Figure 4. Cyclin D1 Is Suppressed by Rapamycin In Vivo in MPNSTs

(A) Western-blot analysis of NPcis tumors. Results shown are typical of all tumors analyzed. Abbreviations: pAKT, AKT phosphorylated at S473; AKT, total AKT.

(B) Western-blot analysis of NPcis tumors. Abbreviations are as follows: IRS1/2, insulin receptor substrate 1/2.

(C) Western-blot analysis of Cyclin D1 expression in lysates from NPcis MPNSTs (upper panel), treated for 8–24 days. Western-blot analysis of p27, c-*myc*, Pdcd4, and p21 expression levels are shown in control and rapamycin-treated tumors (lower panel).

(D) Quantitative RT-PCR expression analysis of Cyclin D1 mRNA isolated from NPcis MPNSTs. The difference in Cyclin D1 mRNA levels is not significant ($p = 0.438$). Error bars represent the SD of RT-PCR values from five treated and untreated samples, performed in triplicate.

(E) Western analysis of Cyclin D1 protein expression in MPNSTs after 1 day of rapamycin treatment (left).Western analysis of Cyclin D1 expression in lysates from NPcis MPNSTs. Abbreviations: Cont., control; Rapa, rapamycin; WD, rapamcyin withdrawal after (right).

(F) Western-blot analysis of Cyclin D1 expression in the human MPNST cell line S462 transduced with either pBabe-puro empty vector (−) or the NF1 GAP-related domain (NF1 GRD) (+).

(G) Western-blot analysis of Cyclin D1 expression in the human MPNST cell line S462 transduced with either pRetroSuper-GFP (shGFP) or pRetroSuper-Cyclin D1 (shCyD1).

(H) Relative proliferative ability of MPNST cell lines expressing either pRetroSuper GFP (shGFP) or pRetroSuper-Cyclin D1 (shCyD1) over a period of 7 days. Error bars represent the SD of cell numbers, counted in triplicate wells.

(I) Western-blot analysis of 3′-HA-tagged-Cyclin D1 expression in the human MPNST cell line S462 transduced with either pBabe-puro empty vector (pBp) or pBabe-puro-3′-HA-Cyclin D1 (CyD1) and treated either with DMSO (−) or 20 nM rapamycin for 48 hr.

(J) Relative proliferative ability of the MPNST cell line S462 expressing either pBabe-puro empty vector (pBp) or pBabe-puro-3′-HA-Cyclin D1 (CyD1) and treated either with DMSO (−) or 20 nM rapamycin for 7 days. Error bars represent the SD of cell numbers, counted in triplicate wells.

findings, FDG uptake would not be expected to be affected by rapamycin in these lesions, suggesting that FDG-PET may not be an appropriate biomarker for all tumor types. More generally, these data suggest that mTOR may contribute to tumorigenesis via distinct effectors in different tumors.

Rapamycin Suppresses TORC1 and Does Not Inhibit or Activate AKT

Two mTOR-containing complexes have been identified in mammalian cells [3]. The TORC1 complex mediates activation of mTOR effectors such as S6K, whereas the TORC2 complex regulates AKT [3]. Although TORC2 has classically been defined as rapamycin insensitive, long-term rapamcyin treatment of some human tumor cell lines inhibits TORC2 and AKT due to the sequestration of nascent mTOR into FKBP12/rapamycin/mTOR complexes [20]. Based on these observations and additional xenograft studies, it is thought that in some tumor types rapamycin may function by suppressing AKT rather than TORC1 [20]. Importantly, however, we found that AKT phosphorylation was not suppressed by rapamycin in any case, even after 30 days of treatment (Figures 4A and 4B), indicating that TORC1 inhibition

mediates the antitumor activity of rapamycin. We also noted that rapamcyin did not generally activate AKT or stabilize IRS proteins (Figure 4B), which has been articulated as a potential therapeutic concern due to the existence of a negative feedback loop emanating from S6K [21, 22].

Rapamycin Suppresses Cyclin D1 Expression in *Nf1* Null MPNSTs In Vivo

Finally, we examined the expression of a panel of the remaining direct and indirect mTOR targets proposed to mediate the effects of rapamycin in other systems including Cyclin D1, PDCD4, myc, p27, and p21 [23, 24]. Surprisingly, the only mTOR target in this list affected by rapamycin in MPNSTS in vivo was Cyclin D1 (Figure 4C). Consistent with reported effects on Cyclin D1 translation, rapamycin had no significant effect on mRNA levels but dramatically inhibited protein expression (Figures 4C and 4D). These results suggested that Cyclin D1 might be one critical target of rapamycin in MPNSTs in vivo. In support of this possibility, reduction of Cyclin D1 was observed within 24 hr of rapamycin treatment in vivo, and rapamycin withdrawal resulted in its re-expression (Figure 4E).

Interestingly, *Nf1* inactivation has been shown previously to enhance Cyclin D1 expression in murine Schwann cells [25]. Moreover, we found that reconstituting human MPNST cells with an active NF1 fragment decreased Cyclin D1 expression, further supporting a connection between these two pathways (Figure 4F). To determine whether suppression of Cyclin D1 could mediate the growth inhibitory effects of rapamycin in this tumor type, Cyclin D1 expression was reduced via shRNA constructs in MPNST cells. Suppression of Cyclin D1 significantly inhibited the proliferation of human MPNST cell lines (Figures 4G and 4H), demonstrating that the proliferation of this tumor type is sensitive to Cyclin D1 levels. However, ectopic expression of Cyclin D1 only slightly ameliorated the growth suppressive effects of rapamycin in vitro (Figures 4I and 4J). These results indicate that although suppression of Cyclin D1 expression is sufficient to significantly inhibit the proliferation of MPNSTs, rapamycin is also likely to be acting on other unidentified mTOR effectors, which may explain its potent cytostatic effects in vivo. Nevertheless, Cyclin D1 has also been implicated as a critical rapamycin target in mantle cell lymphoma (MCL), a tumor type that has been shown to respond to mTOR inhibitors in clinical trials [26], supporting the potential importance of Cyclin D1 as a more general target of mTOR in tumorigenesis.

Taken with previous findings, these data suggest that rapamycin suppresses different tumor types via distinct mechanisms, perhaps distinguished by inhibition of HIF-1α (RCC, PIN), AKT [20], or Cyclin D1 (MCL and MPNST). This heterogeneity should be considered when designing efficacy readouts, particularly as FDG-PET scanning is now being widely incorporated into clinical trials with mTOR inhibitors, but it may not represent a universally accurate biomarker. This point is highly relevant for MPNSTs, which are commonly diagnosed by FDG-PET imaging; however, our results indicate that Cyclin D1 expression may represent a more informative biomarker in this tumor type. In any case these data provide definitive in vivo evidence that mTOR/TORC1 is essential for the pathogenesis of MPNSTs. Furthermore, in addition to providing data to support clinical trials with mTOR inhibitors, these findings provide insight that may be necessary for effective trial design.

Experimental Procedures

NPcis Mice Generation, Treatment, and Measurement of Tumor Volume

C57/BL6 NPcis mice have been previously described [9, 10]. Rapamycin was administered intraperitoneally at 5 mg/kg of body weight, beginning at the time of tumor detection, with 5 days on treatment and 2 days off. Rapamycin (Calbiochem) was initially dissolved in 100% ethanol at a concentration of 25 μg/μl and stored at -20°C. Prior to injection, rapamycin was diluted 1:50 into the vehicle (an aqueous solution composed of 5.2% PEG 400 and 5.2% Triton 80; Sigma). Tumor volume was calculated by measuring length and width of the lesion and with the formula (length) $\times$ (width)^2 $\times$ (0.52). BrdU (10 mg/ml) was injected at a final concentration of 10 μg/g animal weight. BrdU incorporation was quantified as the percent of BrdU-positive cells/number of hematoxylin-stained nuclei. All statistical analyses were done with Student's t test.

Immunoblots, Antibodies, and Retroviral Constructs

Tumor and tissue lysates were normalized and analyzed by immunoblot with the following antibodies as described [6]: total S6 ribosomal protein, phospho-S6 (S235/236), phospho-AKT (S473), and total PARP (Cell Signaling Technology); DcR2 (Stressgen); p53 and IRS1 (Santa Cruz Biotechnology); BrdU (Calbiochem); CD31 and Cyclin D1 (PharMingen); Neurofibromin (Bethyl); HIF-1α (A&G Pharmaceutical); anti-HA tag (Covance); actin (Sigma); IRS-2 (Upstate); anti-Flag tag (Sigma); PDCD4. The following constructs were used: pRetroSuper-GFP (shGFP), CyclinD1 (shCyD1), pBabe-puro HA-tagged Cyclin D1, pBabe-Puro Flag-NF1 Gap-Related Domain (NF1 GRD), which has been previously described [6].

Immunofluorescence and Blood Vessel Density Quantitation

CD31 primary antibody (PharMingen) was incubated 1:50 overnight at room temperature, followed by the secondary antibody (Alexa 594, goat anti-rat IgG, Molecular Probes) for 2 hr (1:500). TUNEL-positive cells were detected with Promega's DeadEnd TUNEL Kit and were costained with Hoechst. For blood vessel density quantitation, images of stained sections were reduced to 4 $\times$ 3 inches (w $\times$ h), and a standard grid (1 cm) was applied to the image. Each box (created by the grid) that displayed CD31-positive cells was counted as 1, and the total number of CD31-positive boxes was determined for the entire image. All statistical analyses were done with Student's t test.

Real-Time PCR

RNA was extracted with Trizol reagent (Invitrogen). Standard curves were generated from a dilution series of RNA isolated from the appropriate untreated control cells. Samples were run in triplicate, and n-fold change was calculated with the following equation: n-fold change = eΔCt, where e = $10^{(-1/\text{slope})}$ and ΔCt is the difference in threshold cycle between samples. Real-time PCR reactions were performed in triplicate using the Assays-on-Demand Taqman Gene Expression Assays from Applied Biosystems and were normalized with an internal control. Probe sets are as follows: Slc2a1 (Glut1) (Mm00441473_m1), Cyclin D1 (Mm00432359_m1), Vegfa (Mm00437304_m1), Vegfb (Mm00442102_m1), Hmox1 (Mm00516004_m1), Edn1 (Mm00438656_m1), and Igfbp3 (Mm00515156_m1).

Cell Proliferation Assay

Cells were plated in the presence of DMSO (Sigma) or rapamycin (20 nM, Calbiochem) at a density of 1.75 $\times$ 10^4 cells per well in 6-well dishes. Cells were counted 24 hr after plating (day 1) and subsequently at day 5 (NIH 3T3 and mouse Schwann cells) or day 7 (all other cell lines). The final time point of each cell line represents the last point prior to reaching confluence.

Supplemental Data

Experimental Procedures and three figures are available at http://www.current-biology.com/cgi/content/full/18/1/56/DC1/.

Acknowledgments

The Pdcd4 antibodies were a generous gift of Dr. Nancy Colburn (National Cancer Institute, U.S. National Institutes of Health, Bethesda, Maryland). pRetroSuper-GFP (shGFP) and Cyclin D1 (shCyD1) were a generous gift of Dr. Daniel S. Peeper (The Netherlands Cancer Institute, Amsterdam, The Netherlands). pBabe-puro HA-tagged Cyclin D1 was a generous gift of Dr. Mark Ewen (Harvard Medical School and Dana-Farber Cancer Institute, Boston, Massachusetts). We thank Scott Plotkin, Pasi Jänne, Alejandro Sweet-Cordero, Brigitte Widemann, Haesun Kim, M. Celeste Simon, and Reuben Shaw for helpful discussions. This work was supported by grant R01 CA111754-01, the Ludwig Center at Dana-Farber/Harvard Cancer Center, and the Children's Tumor Foundation (CTF). C.M.J. was supported in part by a CTF fellowship. B.E.J. was supported in part by the Ludwig Center.

Received: August 7, 2007
Revised: November 6, 2007
Accepted: November 23, 2007
Published online: December 27, 2007

References

1. Ferner, R.E., Huson, S.M., Thomas, N., Moss, C., Willshaw, H., Evans, D.G., Upadhyaya, M., Towers, R., Gleeson, M., Steiger, C., et al. (2007). Guidelines for the diagnosis and management of individuals with neurofibromatosis 1. J. Med. Genet. *44*, 81–88.
2. Martin, G.A., Viskochil, D., Bollag, G., McCabe, P.C., Crosier, W.J., Haubruck, H., Conroy, L., Clark, R., O'Connell, P., Cawthon, R.M., et al. (1990). The GAP-related domain of the neurofibromatosis type 1 gene product interacts with ras p21. Cell *63*, 843–849.
3. Sabatini, D.M. (2006). mTOR and cancer: Insights into a complex relationship. Nat. Rev. Cancer *6*, 729–734.
4. Tonsgard, J.H. (2006). Clinical manifestations and management of neurofibromatosis type 1. Semin. Pediatr. Neurol. *13*, 2–7.
5. Dasgupta, B., Yi, Y., Chen, D.Y., Weber, J.D., and Gutmann, D.H. (2005). Proteomic analysis reveals hyperactivation of the mammalian target of rapamycin pathway in neurofibromatosis 1-associated human and mouse brain tumors. Cancer Res. *65*, 2755–2760.
6. Johannessen, C.M., Reczek, E.E., James, M.F., Brems, H., Legius, E., and Cichowski, K. (2005). The NF1 tumor suppressor critically regulates TSC2 and mTOR. Proc. Natl. Acad. Sci. USA *102*, 8573–8578.
7. Sawyers, C.L. (2003). Will mTOR inhibitors make it as cancer drugs? Cancer Cell *4*, 343–348.
8. Thomas, G.V., Tran, C., Mellinghoff, I.K., Welsbie, D.S., Chan, E., Fueger, B., Czernin, J., and Sawyers, C.L. (2006). Hypoxia-inducible factor determines sensitivity to inhibitors of mTOR in kidney cancer. Nat. Med. *12*, 122–127.
9. Cichowski, K., Shih, T.S., Schmitt, E., Santiago, S., Reilly, K., McLaughlin, M.E., Bronson, R.T., and Jacks, T. (1999). Mouse models of tumor development in neurofibromatosis type 1. Science *286*, 2172–2176.
10. Vogel, K.S., Klesse, L.J., Velasco-Miguel, S., Meyers, K., Rushing, E.J., and Parada, L.F. (1999). Mouse tumor model for neurofibromatosis type 1. Science *286*, 2176–2179.
11. Escudier, B., Szczylik, C., Eisen, T., Stadler, W.M., Schwartz, B., Shan, M., and Bukowski, R.M. (2005). Randomized Phase III trial of the Raf kinase and VEGFR inhibitor sorafenib (BAY 43-9006) in patients with advanced renal cell carcinoma (RCC). J. Clin. Oncol. *23* (*Suppl 16S*), 4510.
12. Demetri, G.D., van Oosterom, A.T., Garrett, C.R., Blackstein, M.E., Shah, M.H., Verweij, J., McArthur, G., Judson, I.R., Heinrich, M.C., Morgan, J.A., et al. (2006). Efficacy and safety of sunitinib in patients with advanced gastrointestinal stromal tumour after failure of imatinib: A randomised controlled trial. Lancet *368*, 1329–1338.
13. Ratain, M.J., Eisen, T., Stadler, W.M., Flaherty, K.T., Kaye, S.B., Rosner, G.L., Gore, M., Desai, A.A., Patnaik, A., Xiong, H.Q., et al. (2006). Phase II placebo-controlled randomized discontinuation trial of sorafenib in patients with metastatic renal cell carcinoma. J. Clin. Oncol. *24*, 2505–2512.
14. Guba, M., von Breitenbuch, P., Steinbauer, M., Koehl, G., Flegel, S., Hornung, M., Bruns, C.J., Zuelke, C., Farkas, S., Anthuber, M., et al. (2002). Rapamycin inhibits primary and metastatic tumor growth by antiangiogenesis: Involvement of vascular endothelial growth factor. Nat. Med. *8*, 128–135.
15. Phung, T.L., Ziv, K., Dabydeen, D., Eyiah-Mensah, G., Riveros, M., Perruzzi, C., Sun, J., Monahan-Earley, R.A., Shiojima, I., Nagy, J.A., et al. (2006). Pathological angiogenesis is induced by sustained Akt signaling and inhibited by rapamycin. Cancer Cell *10*, 159–170.
16. Hudson, C.C., Liu, M., Chiang, G.G., Otterness, D.M., Loomis, D.C., Kaper, F., Giaccia, A.J., and Abraham, R.T. (2002). Regulation of hypoxia-inducible factor 1alpha expression and function by the mammalian target of rapamycin. Mol. Cell. Biol. *22*, 7004–7014.
17. Majumder, P.K., Febbo, P.G., Bikoff, R., Berger, R., Xue, Q., McMahon, L.M., Manola, J., Brugarolas, J., McDonnell, T.J., Golub, T.R., et al. (2004). mTOR inhibition reverses Akt-dependent prostate intraepithelial neoplasia through regulation of apoptotic and HIF-1-dependent pathways. Nat. Med. *10*, 594–601.
18. Pantuck, A.J., Thomas, G., Belldegrun, A.S., and Figlin, R.A. (2006). Mammalian target of rapamycin inhibitors in renal cell carcinoma: Current status and future applications. Semin. Oncol. *33*, 607–613.
19. Brown, R.S., Leung, J.Y., Kison, P.V., Zasadny, K.R., Flint, A., and Wahl, R.L. (1999). Glucose transporters and FDG uptake in untreated primary human non-small cell lung cancer. J. Nucl. Med. *40*, 556–565.
20. Sarbassov, D.D., Ali, S.M., Sengupta, S., Sheen, J.H., Hsu, P.P., Bagley, A.F., Markhard, A.L., and Sabatini, D.M. (2006). Prolonged rapamycin treatment inhibits mTORC2 assembly and Akt/PKB. Mol. Cell *22*, 159–168.
21. O'Reilly, K.E., Rojo, F., She, Q.B., Solit, D., Mills, G.B., Smith, D., Lane, H., Hofmann, F., Hicklin, D.J., Ludwig, D.L., et al. (2006). mTOR inhibition induces upstream receptor tyrosine kinase signaling and activates Akt. Cancer Res. *66*, 1500–1508.
22. Rosen, N., and She, Q.B. (2006). AKT and cancer–is it all mTOR? Cancer Cell *10*, 254–256.
23. Dorrello, N.V., Peschiaroli, A., Guardavaccaro, D., Colburn, N.H., Sherman, N.E., and Pagano, M. (2006). S6K1- and betaTRCP-mediated degradation of PDCD4 promotes protein translation and cell growth. Science *314*, 467–471.
24. Easton, J.B., and Houghton, P.J. (2006). mTOR and cancer therapy. Oncogene *25*, 6436–6446.
25. Kim, H.A., Ratner, N., Roberts, T.M., and Stiles, C.D. (2001). Schwann cell proliferative responses to cAMP and Nf1 are mediated by Cyclin D1. J. Neurosci. *21*, 1110–1116.
26. Costa, L.J. (2007). Aspects of mTOR biology and the use of mTOR inhibitors in non-Hodgkin's lymphoma. Cancer Treat. Rev. *33*, 78–84.